



Influences of structurally-controlled ridge asymmetry on drainage network and divide dynamics

Vincent Godard * ^{1, 2}, Adam M. Forte ³, Martine Simoes ⁴, Carole Petit ⁵, Rodolphe Cattin ⁶

¹Aix Marseille Univ, CNRS, IRD, INRAE, CEREGE, Aix-en-Provence, France, ²Institut Universitaire de France, Paris, France, ³Department of Geology & Geophysics, Louisiana State University, Baton Rouge, USA, ⁴Université Paris Cité, Institut de physique du globe de Paris, CNRS, Paris, France,

⁵Université Côte d'Azur, CNRS, Observatoire de la Côte d'Azur, IRD, Géoazur, Valbonne, France, ⁶Géosciences Montpellier, Université de Montpellier, CNRS, Montpellier, France

Author contributions: Conceptualization: VG. Methodology: VG. Software: VG. Validation: VG,AF,MS,CP,RC. Formal Analysis: VG,AF,MS,CP,RC. Investigation: VG,AF,MS,CP,RC. Resources: VG. Writing - original draft: VG. Writing - Review & Editing: VG,AF,MS,CP,RC.

Abstract Asymmetric morphologies are ubiquitous in many landscapes, but the influence of tectonics, climate or bedrock properties on the development and persistence of this asymmetry is difficult to assess. This study investigates the implications of structurally-controlled relief asymmetry on drainage divide dynamics and network organization. We focus on the French Southern Alps, a tectonically quiescent region where Eocene and Miocene thin-skinned deformation of a well-developed Mesozoic sedimentary series is still strongly imprinted in present-day landscape form, in particular through the presence of asymmetric ridges with steep cliff faces opposite to gently dipping structural surfaces. We build a dataset combining systematic measurements of geomorphological properties of these ridges with available geological information about strata dip direction, to identify eventual systematic correlations between metrics characterizing divide morphology and instability and the structural configuration of the ridge, from a local scale to the larger organization of the river network. We observe a systematic tendency for aggressor basins, according to the χ metric and local slope contrasts, to be located opposite to the dip direction of the strata, with respect to the divide. Such configuration arose from the initial structural asymmetry of the layered landscape, but we propose that it has been maintained over time by an inhibition of fluvial or hillslope erosion processes on the steepest and up-dip sides of the divide. Such phenomena can have strong implications on the transient evolution of the planform drainage structure, by allowing the persistence of out-of-equilibrium configurations over extended periods of time.

Non-technical summary River networks are dynamic systems and the shape of river basins evolve through time, with major implications for the evolution of topographic relief, climate or ecosystems. A key process in this evolution is the migration of drainage divides allowing one basin to grow at the expense of another adjacent basin. In landscapes developing over deformed sedimentary series, it is a common situation for these divides to be asymmetric with a steep cliff on one side and a gentler sloping surface on the other following the dip of the sedimentary series. We investigate the possible control of this topographic asymmetry on the migration of drainage divides in the French Southern Alps. We observe that the basins with more potential to grow at the expense of their neighbor(s) are more likely to be located on the side of the divide opposite to the dip direction of the strata. One explanation for this configuration is that the landscape is still in a disequilibrated configuration, due to a slowing-down of erosion processes on the steep sides of the divides. While such behavior could appear counter-intuitive, we discuss a series of geomorphological processes which could contribute to this situation, and keep landscapes away from equilibrium conditions over geological time scales.

1 Introduction

External forcing such as tectonics or climate, as well as internal properties such as bedrock lithology, dictate the structure and evolution of landscapes (e.g. Whipple, 2009; Whittaker, 2012). Intensive research efforts have aimed at understanding how fluvial incision and hillslope erosion processes create, maintain, and dissipate topographic relief. These studies have led to a better understanding of the processes that influence the vertical development of landscapes and how they control the characteristics of fluvial and hillslope reliefs uplifted above their base level (Tucker and Whipple, 2002).

However, the impact of fluvial dynamics on landscapes is not limited to along-stream vertical incision, but also includes the horizontal structure of river networks and the processes that drive its evolution over time (Clark et al., 2004; Pelletier, 2004; Perron et al., 2008; Stark, 2010; Bonnet, 2009; Perron et al., 2012; Zhou et al., 2022; Zhou and Tan, 2023; Zhou et al., 2022). These planform dynamics of fluvial systems are much less understood than the vertical incision associated with fluvial processes.

The migration of watershed divides, through the capture of part of one basin area by another, either progressively or by discrete events, is one of the most important controls on the network scale evolution of drainage

Received:
April 12, 2024
Accepted:
January 18, 2025
Published:
March 11, 2025

Editor-in-Chief:
Alice Lefebvre
Associate Editors:
Olutoyin Fashae
Anonymous AE2
Managing Editor:
Helen Dias
Copy Editor:
Anatolii Tsypalenkov

Reviewers:
Anonymous
Anonymous

The work is licensed under CC BY 4.0 International.

*Corresponding author: godard@cerege.fr

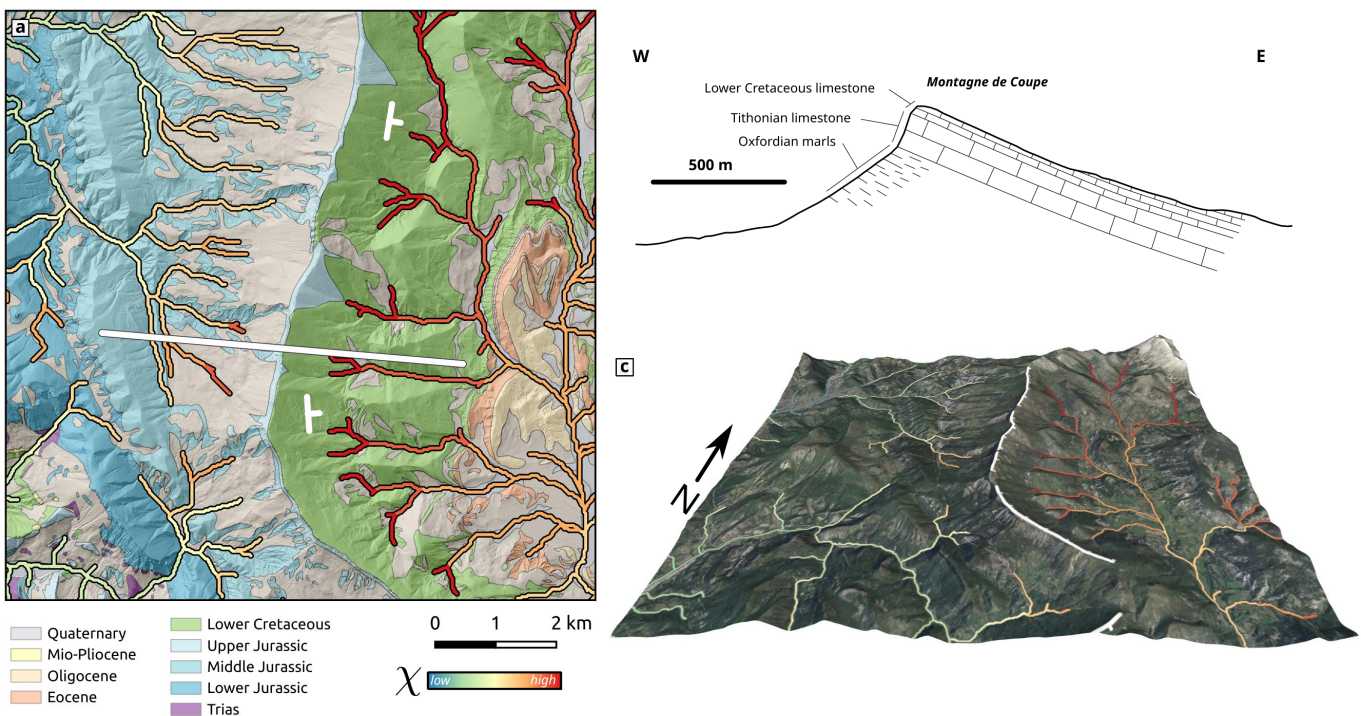


Figure 1 Example of the Montagne de Coupe ridge, South-Eastern France (see location on Fig. 2b) (a) Harmonized BRGM 1/50000 geological map (accessible through BRGM WMS). River network is colored according to χ values. Thick white line indicates the location of the topographic cross-section. Dip directions along the ridge are also reported. (b) Topographic and simplified geological cross-section. (c) Oblique view with IGN orthophotos and river network.

systems, with far-reaching implications. From a morphological point of view, it sets the locations of active erosion, sediment fluxes through watersheds, and where dissection of relief occurs (e.g. Willett et al., 2014; Whipple et al., 2016; Forte and Whipple, 2018; Dahlquist et al., 2018; Vacherat et al., 2018; Sassolas-Serrayet et al., 2019; Schwanghart and Scherler, 2020; Rohrmann et al., 2023). It has also been proposed that this dynamics of watershed divide migration could play a major role in the continental-scale evolution of ecosystems, particularly aquatic ecosystems, and could be one of the fundamental processes driving the distribution of biodiversity (e.g. Waters et al., 2001; Gallen, 2018; Lyons et al., 2020; Val et al., 2022; Cassemiro et al., 2023). Therefore, a better comprehension of the processes controlling divide migration, and resulting river network organization, is essential for the understanding of many phenomena that affect the Earth's surface and the critical zone.

As for many processes driven by fluvial incision, the migration dynamics of watersheds is strongly influenced by climatic and tectonic factors. Recently, the importance of bedrock lithology on migration dynamics has also been demonstrated in numerical models (Forte et al., 2016; Mitchell and Forte, 2023) and field studies (Gallen, 2018; García-Delgado et al., 2023). Lithology, which is incorporated through the erodibility parameter in most fluvial incision models, is a critical factor in influencing fluvial incision, although it is challenging to quantify effectively (e.g. Lavé and Avouac, 2001; Godard et al., 2010; Bursztyk et al., 2015; Small et al., 2015; Zondervan et al., 2020). It also appears that lithology contrasts related to underlying geological structures can have a lasting impact on the evolution of

watershed boundaries by influencing capture processes (Ward, 2019; García-Delgado et al., 2023).

Sedimentary series undergoing thin-skinned deformation are prevalent in the external domains of many mountain ranges. These layered lithologies are highly anisotropic for a wide range of tectonic and surface processes. In particular, they are often associated with asymmetric reliefs, which are common features of both tectonically active and inactive fold and thrust ranges. Such asymmetry is usually of structural origin, and associated with the uplift of the range along ramp-flat systems or with the development of asymmetric propagation folds. The resulting topography often exhibits a significant difference in slope across ridges, as maintained by tectonic uplift when active, and controlled by the dip direction of underlying strata. The steeper side, which can display bare bedrock cliffs, is most often opposed to the dip direction, whereas a gentler sloping surface on the other side often follows a structural surface set by the dipping strata (Fig. 1).

This difference in slopes across ridges and associated drainage divides is structurally-controlled and of tectonic origin, and is present since the formation of the ridge, independently of ulterior climatic and geomorphic forcing on the landscape. The asymmetry can induce very contrasted processes and evolution on the two sides, with for example a steep cliff dominated by rock falls on one side, and a gently dipping soil-mantled surface dominated by creep on the other side. Similarly, weathering processes can act at very different paces depending on the respective depths, on each side, of the regolith overlaying bedrock. Such drastic differences in processes between the two sides can have significant implications on how the hillslopes and first-order chan-

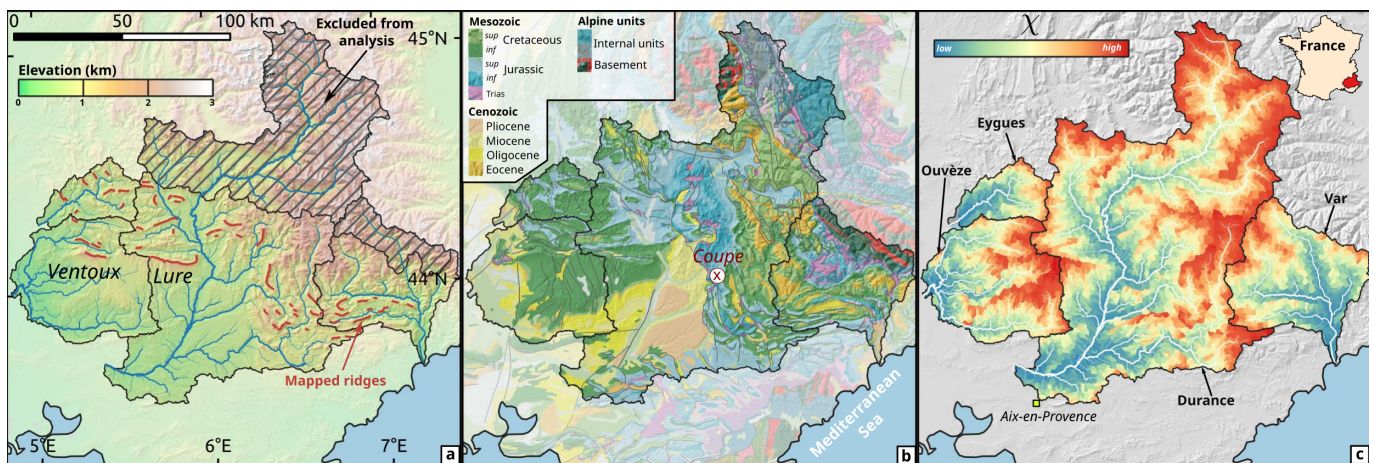


Figure 2 Situation maps for the studied area in the French Southern Alps. (a) Topography, river network and limits of the studied major basins. Hatched area in the upper part of the Durance and Var catchments was excluded from the analysis due to important glacial imprint. Red lines are mapped homoclinal ridges, where the dip direction of the strata could be clearly determined. (b) Geological map ($1/10^6$ BRGM). Marker x corresponds to the location of interest presented on Fig. 1. (c) χ map ($\theta = 0.5$). Integration starting points are at the outlets of each basin.

nels of these ridges respond. In particular, the dynamics of divide migration, where a basin captures part of the drainage area of another, can be modulated by differences in the erosion processes and their response timescales between the two sides of the divide (Whipple et al., 2017; Braun, 2018). In turn, these local processes, at the local scale of the ridge and associated divides, may impact the way the river network adjusts.

At first approximation, these differences in slope are expected to result in differential erosion rates and promote drainage divide migration in the direction opposite the steeper side. All metrics measured in the proximity of the divide, such as relief, channel steepness, should be consistent with this disequilibrium and direction of migration. One interesting aspect of this asymmetry and corresponding direction of migration, is that it does not, *a priori*, reflect network scale dynamics and competition between adjacent catchments, but is defined by the *ab initio* local structural geometry of the ridges. One could wonder how these local dynamics interact with network scale forcing, propagating along river networks, at the scale of 10s of km. In particular, whether or not the topographic metrics characterizing the larger scale planform dynamics of river networks will display drainage direction patterns consistent with the locally controlled ridge metrics remains to be determined. The χ metric has, for example, been a widely used tool to identify such large-scale geometrically out-of-equilibrium drainage configurations, and to derive directions of drainage migration (Willett et al., 2014). In settings with complex geology and tectonic history, we could expect to observe χ contrasts across ridges indicating long wavelength landscape disequilibrium, but with no specific overall preferential orientation across ridges with respect to their initial topographic asymmetry, which is a local attribute. How these two length scales (large-scale planform river network vs. local asymmetry of ridges) interact in dictating landscape evolution in deformed layered sedimentary terrains is still poorly understood and requires a systematic morphological analysis.

To explore these questions, we investigate the impli-

cations of initial relief asymmetry, induced by structures and layered stratigraphy, on drainage divide dynamics in the French Southern Alps. In this region, thin-skinned deformation of a well-developed Mesozoic sedimentary series has strongly imprinted the landscape, with widespread occurrences of asymmetric ridges. This landscape is presently affected by negligible, possibly only local, active deformation, and the shortening that formed the observed asymmetric ridges occurred mostly during Eocene and Miocene tectonic phases (Walpersdorf et al., 2015; Godard et al., 2020; Bestani et al., 2016). The climatic conditions can also be considered to be relatively homogeneous over the studied region. We take advantage of this situation, where active tectonics can be neglected, to study the relaxation of such initially structurally-controlled landscape toward planform equilibrium. We build a dataset combining systematic measurements of the local geomorphological properties of ridges with available geological information about strata dip direction, to identify eventual systematic correlations between topographic metrics characterizing divide instability and the geological configuration of the ridges, both at the local scale of the ridges and of the larger river network.

2 Settings

Our study area is located in the southern part of the French Alps, adjacent to the northern ranges of Provence (Fig. 2). The landscapes of this region are characterized by wide valleys and mountain ranges that can reach altitudes between 2000 and 3000 meters. Most of the ranges in these areas were formed during the Pyrenean deformation phase in the Eocene, followed by Alpine deformation in the Miocene (Mollieix et al., 2011; Bestani et al., 2016). The influence of the Pyrenean deformation is especially pronounced in the southern part of the Provence sector, mainly expressed by the dominance of east-west oriented mountain ranges.

We are focusing on four main watersheds that drain the topography of this area : the basins of the Eygues, Ouvèze, Durance, and Var rivers. The largest of these

basins is the Durance, which is the primary tributary of the Rhône in its downstream part. For the Durance and Var basins, the upstream areas were occupied by glaciers during the last glacial cycle, which had significantly impacted the corresponding valleys' morphologies. These areas will not be considered in the analysis carried out in this study (Fig. 2a).

The geology of the studied area is largely dominated by Mesozoic sediments (Fig. 2b), primarily Jurassic and Cretaceous, deposited within the context of an epicontinental platform (Léonide et al., 2007; Leonide et al., 2012). This Mesozoic sedimentation is dominated by carbonates, with locally more marly sequences. Very massive limestone beds associated, for instance, with the sedimentation of the Lower Cretaceous or the terminal Jurassic, play a crucial role in shaping the relief and forming highly distinctive cliffs in the landscape. The early Alpine history of the region is also characterized by detrital deposits such as flysch sequences in the northern part of the studied area.

These platform deposits were subsequently deformed during the Eocene terminal north-south convergence phase of the Pyrenean orogeny. Most of the relief in Provence was formed during this deformation phase. The Alpine deformation then overprinted these earlier phases during the Miocene, and is particularly well expressed in the southern Alps (Espurt et al., 2012; Bestani et al., 2016). The Alpine deformation phase was also associated with significant erosion of the newly formed topography, and molasse-type sedimentation occurred in the Valensole basin during the Miocene and Pliocene (Clauzon et al., 1989). The Messinian salinity crisis affected the hydrographic networks of the Rhône and Durance rivers, along several hundred kilometers upstream of the Mediterranean (Hsü et al., 1977). The canyons formed during this event were subsequently filled with detrital sediment when the sea returned at the end of the crisis (Clauzon et al., 2011). The last stage of landscape evolution corresponds to the major glacial cycles of the Quaternary period, involving the widening of the upstream parts of valleys and a phase of incision in the molasse deposition zones around 1 million years ago. Active deformation is presently very limited (Nocquet et al., 2016), and recent fault slip has been identified only locally on some structures (Hippolyte and Dumont, 2000; Godard et al., 2020). Even though Quaternary glaciations in the upstream portion of the drainage basins induced significant downstream fluvial incision, it is clear that the bulk landscape structure of the Provence and peri-Alpine ranges was acquired before the Pliocene (Bestani et al., 2016) and has been since mostly relaxing.

Structurally and stratigraphically-controlled topographic asymmetry in fold-and-thrust belts could arise from various mechanisms. They can develop from thrust sequences on nearly monoclonal strata, or from the erosion of asymmetric anticlines with a steep and a gently dipping limb (Fig. 1b). In most of the western Provence domain, the structural style of the Mesozoic series is controlled by the existence of a thick lower Cretaceous Ugonian limestone unit, which promotes the former type of deformation. In contrast, the oc-

currence of pronounced asymmetric folds will be more common north of the Ventoux-Lure axis (Fig. 2a), where the lower Cretaceous facies are different.

The result of this complex geological history is the existence of a system of mountain ranges with varied orientations, primarily constituted of Mesozoic carbonate sediments. Many of these mountain ranges display a first-order structural control and exhibit a morphological asymmetry between their two flanks, linked to the dip direction of the strata (Fig. 1). The widespread occurrences of such configuration makes it an interesting location for analyzing the interactions between local geology and the dynamics of fluvial networks in a relaxing landscape.

3 Methods

We present here the methods used to extract the ridges of the landscape and to assess their degree of instability using different morphometric criteria. We present first the general concepts underlying the use of these metrics, and then their implementation in our area of interest.

3.1 Concepts

River incision I ($[LT^{-1}]$) is often described using the simple stream power formulation using along-channel slope S and drainage area A ($[L^2]$), such as,

$$I = KA^m S^n, \quad (1)$$

where K is an erodibility coefficient ($[L^{1-2m}T^{-1}]$), and m and n are empirical exponents (Howard, 1994; Whipple and Tucker, 1999). Under steady-state conditions river incision I equals rock uplift U and equation 1 can be reorganized as,

$$\begin{aligned} S &= \left| \frac{dz}{dx} \right| \\ &= \left(\frac{U}{K} \right)^{\frac{1}{n}} A^{-\frac{m}{n}}. \end{aligned} \quad (2)$$

Equation 2 can be integrated from base level, at position x_b , to x (Perron and Royden, 2013) as,

$$z(x) - z(x_b) = \int_{x_b}^x \left(\frac{U}{KA^m} \right)^{\frac{1}{n}} dx. \quad (3)$$

Under the assumption that U and K are spatially constant, equation 3 becomes,

$$z(x) = z(x_b) + \left(\frac{U}{KA_0^m} \right)^{\frac{1}{n}} \chi, \quad (4)$$

where A_0 is a reference drainage area (Perron and Royden, 2013), and with,

$$\chi = \int_{x_b}^x \left(\frac{A_0}{A} \right)^{\frac{m}{n}} dx. \quad (5)$$

Equation 5 relates the metric χ , which depends only on the river network configuration, to steady state river

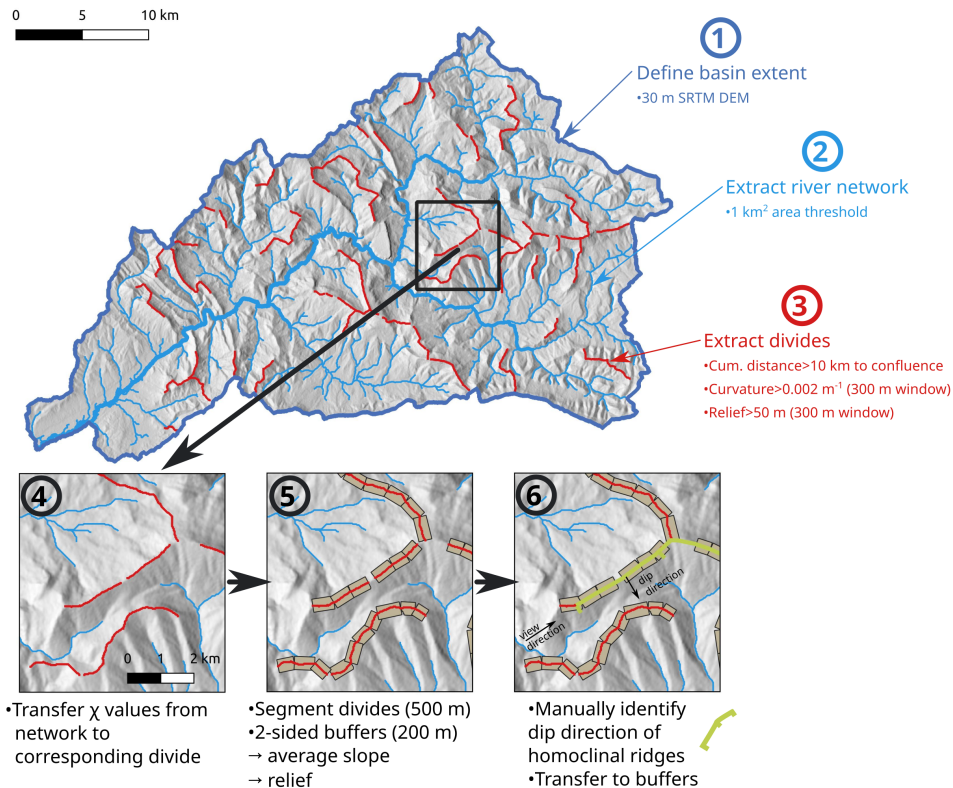


Figure 3 Description of the workflow used to extract and process data associated with divides. See text for details.

channel elevation. Under the assumption of spatially uniform lithology and uplift rates, differences in χ across a drainage divide can be interpreted as the expression of a disequilibrium in the planar organization of the river network (Willett et al., 2014; Whipple et al., 2017; Forte and Whipple, 2018; Habousha et al., 2023), and can be used to infer the possible direction of drainage divide migration as a response to this disequilibrium. In the case of spatially variable lithology or uplift rates, χ contrasts across a divide may not reflect current divide motion, but instead reflect the expected behavior of the divide if the spatial variability in lithology or uplift rates were removed (e.g. Forte and Whipple, 2018).

The χ parameter reflects the network scale organization of the river network and associated instabilities (Willett et al., 2014). While it can provide first order information on divide dynamics, the results' robustness can be strongly affected by the complexities and spatial variability of tectonics, lithological and geomorphological conditions along the integration path (e.g. Gailleton et al., 2021). Topographic gradients and relief are primary drivers of erosion in most settings (e.g. Montgomery and Brandon, 2002; Ouimet et al., 2009), and can be used as proxies for relative variations of erosion rates. Cross-divide contrasts in these topographic properties can be considered to reflect similarly oriented contrasts in erosion rates. For that reason, they can be used to unravel the potential migration directions due to differential erosion acting in the direct vicinity of the ridges. This approach to assess the potential instabilities at the local scale of an individual ridge specifically focuses on cross-divide differences in hillslope

and first-order channels geomorphological properties. These properties, referred to as Gilbert metrics, are for example the topographic gradient and local relief in the direct neighborhood of the divide (Forte and Whipple, 2018). Computation of these metrics is straightforward from a Digital Elevation Model, once the divides have been identified. This type of divide stability analysis provides a local view on the active processes acting directly on both sides of a divide, whereas χ contrasts analysis is rather focused on the longer wavelength stability of the drainage network.

3.2 Implementation

A database for ridge segments was constituted for four major rivers basins in SE France: Durance, Var, Eygues and Ouvèze (Fig. 2). All processing was carried out using IGN-BDALTI 25 m resolution Digital Elevation Model (DEM). The calculations were carried out using the R software (R Core Team, 2023) with the terra (Hijmans, 2023) and rgrass (Bivand, 2023) packages as well as GRASS GIS (GRASS Development Team, 2022). We first extracted the river network and basin limits from the DEM, using an area threshold of 1 km² for the initiation of channels (Fig. 3). This value is large enough to be sure to extract clearly channelized portions of the topography. χ values were computed along the network starting from each basin outlet, using a concavity of 0.5, which is close to the widely reported average for this parameter, and a normalizing area A_0 of 1 km². Choosing other values for these parameters will change the absolute value of χ , but is unlikely to affect the nature of the direction of differences across divides. Note that in the following, all χ comparisons across ridges will be car-

ried out within the same basin, as we do not compare χ values across the ridges delineating the drainage divides between the four studied catchments, in order to avoid inconsistencies associated with the different outlet starting points for the integration pathways (Forte and Whipple, 2018).

The intra-catchment divide network was also extracted, and divide segments were defined such that each segment is associated with a unique couple of opposite first-order drainages. We filtered the divide network based on various criteria, to retain divide segments corresponding to important and prominent ridges. We discarded all divide segments where the local relief and curvature computed over a 300 m diameter window were below 50 m and 0.002 m^{-1} , respectively. The size of the window is large enough to encompass the hilltop and a significant portion of the hill-sides on both sides. The threshold values for curvature and relief allow restricting the dataset to well-defined and prominent ridges. We computed the combined distance to the common confluence, calculated from both sides of each divide segment. We retained only the divide segments where this distance was higher than 10 km. By doing so, we were able to focus our analysis on the main divides associated with the range crests, and set aside the less important divides between first-order basins draining the same flanks of the ranges. It allows us to focus on the network scale organization of the network, and avoid small-scale interactions between adjacent basins. We also excluded from the analysis all the divides located in the northern areas of the Durance and Var catchments, which were strongly affected by Late Quaternary glaciations. We also restricted our analysis to the divides over Mesozoic terrains, constituting most of the relief deformed during Pyrenean and Alpine orogenies.

χ values of first-order drainages from both sides were transferred to the divide segments. In order to facilitate the following analysis of the dataset, divide segments were then split into homogeneous sub-segments of 500 m in length. On each side of the divide, 200 m-wide buffers were delineated for each sub-segments, and zonal statistics such as average slope and relief were computed over these buffers. Slope is computed at each pixel in the steepest drainage direction toward the neighboring pixels. The size of the buffer is chosen to be large enough to sample a significant portion of the hillside, and small enough to avoid interactions with the fluvial network. These statistics were transferred as attributes to the divide sub-segments, with a clear distinction between the two different sides.

Using BRGM 1/50000 geological maps and IGN BD-ORTHO air photos, we identified dip directions of Mesozoic geological strata with respect to the sides of the divide sub-segments.

The final result of our processing workflow is a vector of divide sub-segments, with an attribute table containing information about χ , slope and relief from both sides of the divide and, when this information could be retrieved, the dip direction of the underlying strata. In most of the analysis carried out on this dataset, the cross-divide differences in geomorphological parame-

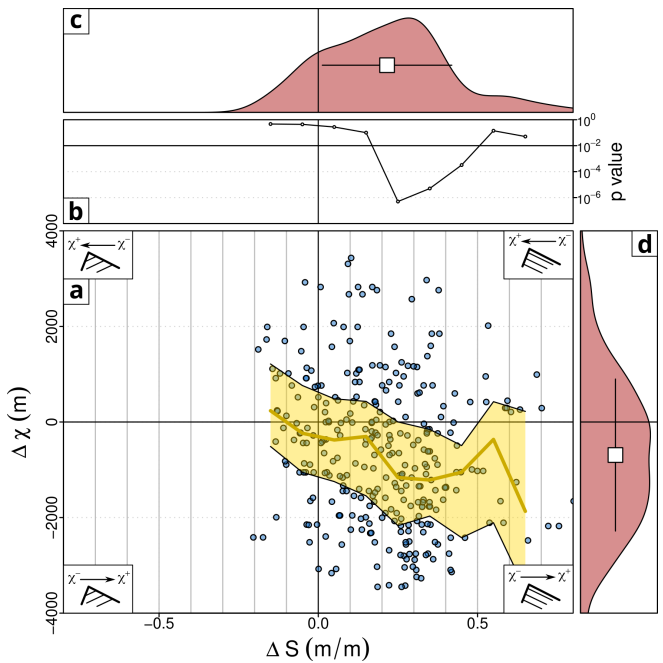


Figure 4 Analysis of the relationship between $\Delta\chi$ and ΔS across ridges identified on Fig. 2a. For all the analyses presented here, ridges are selected according to the following criteria in terms of prominence : the local relief (300 m window) must be higher than 50 m and the curvature higher than $2 \times 10^{-3} \text{ m}^{-1}$, and the combined distances from both sides of the ridge to the common confluence are higher than 10 km. We only consider the Mesozoic sedimentary cover. Dip directions of the strata were identified from DEM, orthophotos and 1/50000 BRGM geological maps. See Fig. 3 for a description of the process. (a) Each point represents a ~ 500 m long ridge segment. The differences in χ and S across the ridges are computed in the sense of the dip direction. Bold yellow line is the median computed over 0.1 m/m-width bins and the shaded area is the interquartile range. (b) p-values for a one sample t-test (H_1 : mean of $\Delta\chi \neq 0$) for each bin. (c) Distribution of ΔS values, square and error bar indicate mean and standard deviation. (d) Distribution of $\Delta\chi$ values, square and error bar indicate mean and standard deviation.

ters (χ , slope, relief) are computed following the dip direction : $\Delta\chi = \chi_{\text{updip}} - \chi_{\text{downdip}}$. When dip-direction is unavailable, cross-divide differences are computed starting from the steepest side.

4 Results

In many settings, structurally controlled relief implies the existence of an asymmetry between the two sides of a divide, with a steep high-relief cliff on one side and a gentler slope in the dip direction on the other side, where the surface gradient is often set by the dip angle of the strata (Fig. 1). This relationship between geological structures and topographic asymmetry is consistent with the observations in our data set in terms of slope ($\Delta S > 0$ in Figs. 4a and 4c) or relief ($\Delta R > 0$ on Figs. 5a and 5c).

We also observe a χ asymmetry predicting migration from the high-slope/relief toward the low-slope/relief side of the divide (Figs. 4d and 5d), which would *a priori* be consistent with the definition of Gilbert metrics and the dynamics observed in many Landscape Evolution Models. This corresponds to negative $\Delta\chi$ values, as we compute the cross-divide difference starting from the steepest updip side. It is important to keep in mind that, in relief generated by thin-skinned deformation,

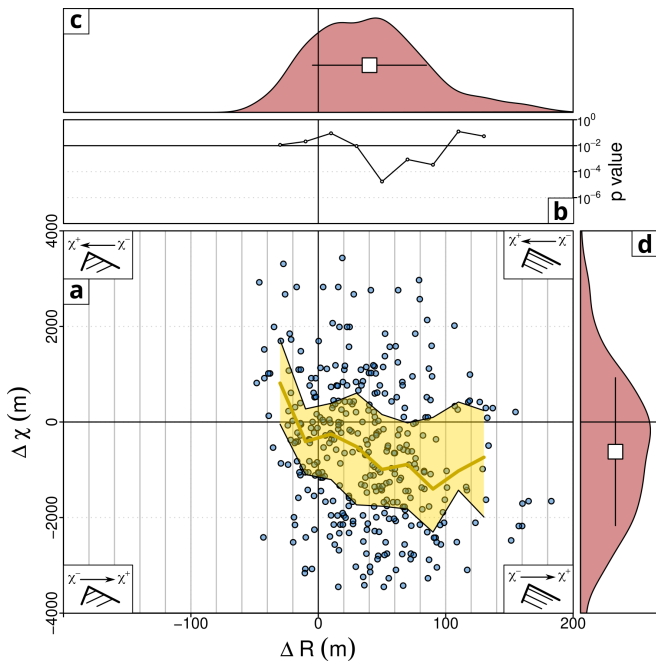


Figure 5 Analysis of the relationship between $\Delta\chi$ and difference in relief ΔR across ridges identified on Fig. 2a. The dataset is the same as the one presented on Fig. 4, obtained with the method presented on Fig. 3. Relief R is computed over the buffers centered on the ridge lines (200 m half-width). (a) Each point represents a ~500 m long ridge segment. The differences in χ and relief across the ridges are computed in the sense of the dip direction. Bold yellow line is the median computed over 20 m-width bins and the shaded area is the interquartile range. (b) p-values for a one sample t-test (H_1 : mean of $\Delta\chi \neq 0$) for each bin. (c) Distribution of ΔR values, square and error bar indicate mean and standard deviation. (d) Distribution of $\Delta\chi$ values, square and error bar indicate mean and standard deviation.

the topographic asymmetry across a ridge is often a direct expression of the initial tectonic deformation pattern, and acquired early in the formation of the landscape. In particular, this asymmetry is not primarily a morphological response to differential erosion across the divides resulting from different base level lowering rates in the catchments from each sides.

The key observation in our dataset is that the $\Delta\chi$ distribution of asymmetric ridges ($\Delta S > 0.2$) is not centered on zero, and that there is a statistically significant tendency for low χ values (aggressor basins) to be located on the side of the divide opposite to the dip direction of the strata (Figs. 4 and 5). Such systematic relationship between the χ asymmetry across the divide and the geological configuration of the ridge suggests a structural control on drainage divide evolution, possibly through a modulation of erosion processes delaying the migration of the divide toward a planar equilibrium configuration of the river network. Using other metrics, such as the Divide Asymmetry Index (DAI) proposed by Scherler and Schwanghart (2020) (Fig. 6), we find a tendency similar to that identified on Figs. 4 and 5, which is that the aggressor basin is located on the steep side of the divide and opposite to the dip direction.

We split the dataset according to the combined distance to the common confluence for drainages originating from both sides of the ridge segments (Fig. 7). This distance to confluence can be used as a metric to order ridges in terms of their importance in the net-

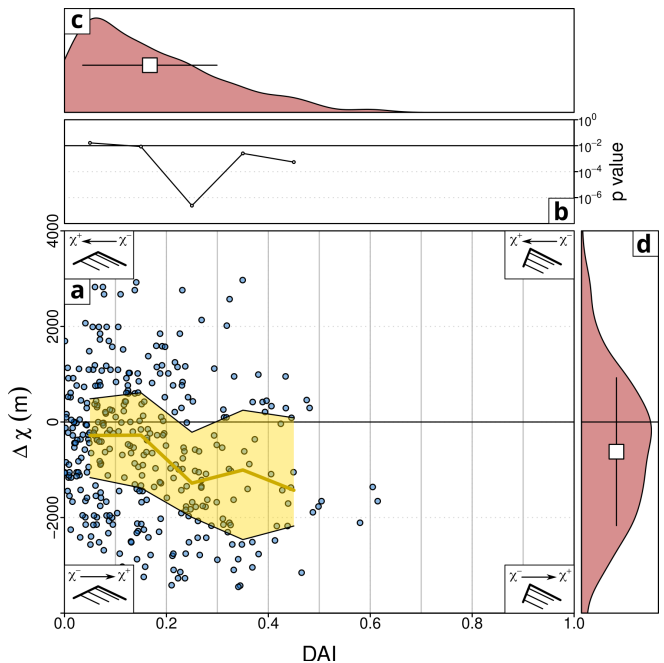


Figure 6 Analysis of the relationship between $\Delta\chi$ and Divide Asymmetry Index (DAI) (Scherler and Schwanghart, 2020) across ridges identified on Fig. 2a. The dataset is the same as the one presented on Fig. 4, obtained with the method presented on Fig. 3. $DAI = |\frac{\Delta R}{\Sigma R}|$, where relief R is computed over the buffers centered on the ridge lines (200 m half-width). (a) Each point represents a ~500 m long ridge segment. The differences in χ across the ridges are computed in the sense of the dip direction. Bold yellow line is the median computed over 0.1-width bins and the shaded area is the interquartile range. (b) p-values for a one sample t-test (H_1 : mean of $\Delta\chi \neq 0$) for each bin. (c) Distribution of DAI values, square and error bar indicate mean and standard deviation. (d) Distribution of $\Delta\chi$ values, square and error bar indicate mean and standard deviation.

work scale landscape structure (Scherler and Schwanghart, 2020), and defining these different subgroups allows separating the short- and long-wavelength dynamics of the landscape. If dip direction did not influence drainage divide dynamics, we would expect all distributions to be centered on $\Delta\chi = 0$. On the contrary, the global distribution is offset with respect to $\Delta\chi = 0$ with a negative mean $\Delta\chi < 0$ as already observed in Figs. 4 to 6. In the distance subgroups, the $\Delta\chi$ offset increases with the combined distance to confluence, so that ridges with long flow paths between their sides are more likely to display aggressor basins on the side opposite to the dip direction. The existence of more asymmetric divides for long distances to confluence supports the idea that the local structural control we are investigating is an important control on the network scale organization and on the evolution of the river network. One could argue that increasing the distance to confluence corresponds to longer integration paths for the calculation of χ , which might contribute to increase the variability between the two sides and the range in $\Delta\chi$ values computed across the ridges. We underline that we observe this effect in our dataset with an increase in the standard deviation of $\Delta\chi$ with distance to confluence (Fig. 7), and, again, that the key observation we make, supporting a structural control, is instead the systematic $\Delta\chi < 0$, as the cross-divide difference in χ is computed in the dip direction.

The data analyzed above (Figs. 4 to 6) is restricted to

the limited number of ridges where the dip direction of the strata could be determined from visual analysis of geological maps or aerial photographs. We also analyze χ contrasts (here referred as $\Delta\chi$ due to the differences in the calculation convention) across all ridges extracted from the DEM and compare with the ones where the dip direction was determined (Fig. 8). For all ridges (solid grey in Fig. 8) the distribution appears to be centered on 0, with slight skewness, which suggest an overall equilibrated configuration for the planar structure of the river network in this area. For all ridges with a significant slope asymmetry ($|\Delta S| > 0.2$) there is a corresponding χ asymmetry, with aggressor drainages more likely to be located in front of the steepest side. This effect is more pronounced for structurally controlled ridges (homoclinal, in blue in Fig. 8) than for the whole dataset, which again reinforces the idea of a structural control on drainage migration dynamics.

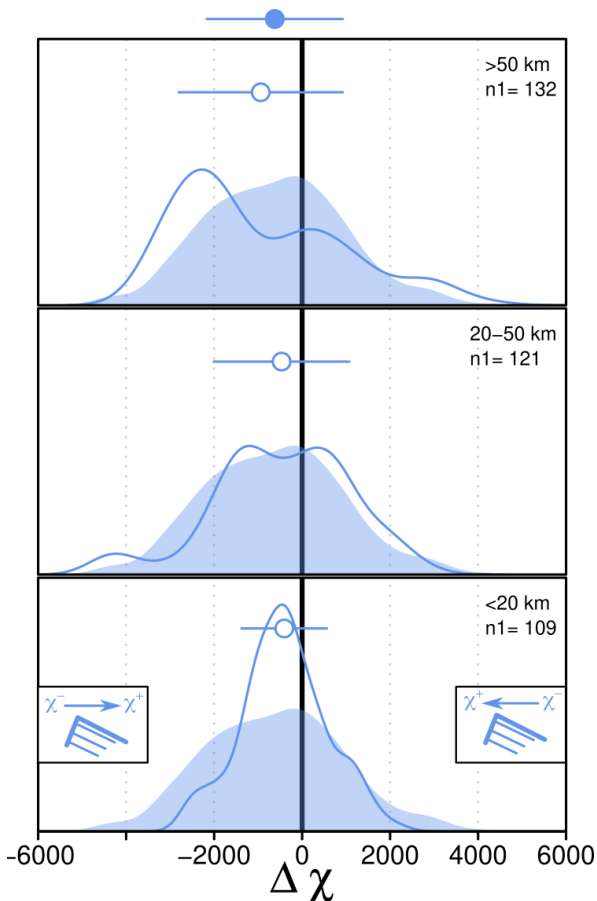


Figure 7 Kernel density estimate distributions of cross divide differences in χ ($\Delta\chi$, with difference computed according to the dip direction) for different values of the combined distance to common confluence (Fig. 3). Filled distributions correspond to all data presented on Fig. 4, with filled circle and error bar on top of the plot indicating the mean and $\pm 1\sigma$. Solid lines correspond to subsets according to the added distances from both sides of the ridge to the common confluence. Open circles and error bars correspond to mean and $\pm 1\sigma$ for these subsets. On all plots the Y-axis is the estimated density, whose exact value has no particular significance.

5 Discussion

5.1 Possible methodological limitations

From a methodological point of view, there are classical limitations on the computation of the χ metrics that similarly apply to our study. One of the key assumptions behind the χ calculation is the homogeneity of tectonic and lithological conditions along the river on which the integration is performed from downstream to upstream (Perron and Royden, 2013). Although primarily sedimentary, the lithologies in the area we consider are highly variable, alternating and juxtaposing carbonates and marls, as well as detrital sediments. Furthermore, the last major tectonic phase dates back to the Miocene, but the possibility of tectonic reactivation, particularly locally at the Alpine front, cannot be ruled out (Godard et al., 2020). Finally, it is important to note that, by definition, the calculation of χ is based on the stream power formalism, which considers detachment-limited incision. However, the conditions of many of the major rivers in our study area are likely hybrid, with some regions exhibiting dynamics closer to transport-limited processes. Similarly, we postulate that the concavity $\theta = 0.5$ of the rivers is constant across the study area, whereas spatial changes could affect the computation of χ . Nevertheless, despite the variability in lithological, tectonic, and process parameters, which can significantly influence the χ calculation (Gailleton et al., 2021), we do observe in this study a systematic asymmetry in this metrics along the ridges whose morphologies are structurally controlled. If the natural variability mentioned above was the first order control on computed χ values, we would expect that these disturbances and variations along the watercourse would lead to a random distribution of χ values across the divides, and that the $\Delta\chi$ values would display a symmetric distribution centered around 0 for all ΔS bins in Figs. 4 to 6.

Additionally, one could argue that the differences in χ observed across the asymmetric ridges arise geometrically due to the difference in flank lengths between the two sides of the structurally-controlled ridge, even though the channel initiation threshold area considered here is large enough to limit such influence. If this were the case, we would expect to observe more pronounced χ contrasts for shorter distances to the confluence between the streams originating from both sides of the ridge (Fig. 7), where this geometric effect would dominate the signal. In fact, our data display the opposite tendency, with higher χ contrasts for longer distances to confluence. This supports the idea that the signal we observe is not at first-order controlled by the channel network configuration near the ridges, but that there is a larger-scale imprint on the landscape and channel organization.

Finally, another point of caution is the climatic history of the region. We intentionally excluded a substantial part of the upstream areas of the studied watersheds in order to eliminate the zones that were directly impacted by glaciers. Nevertheless, it is possible that glacial or periglacial processes may have had differential influences across the divides, especially for east-

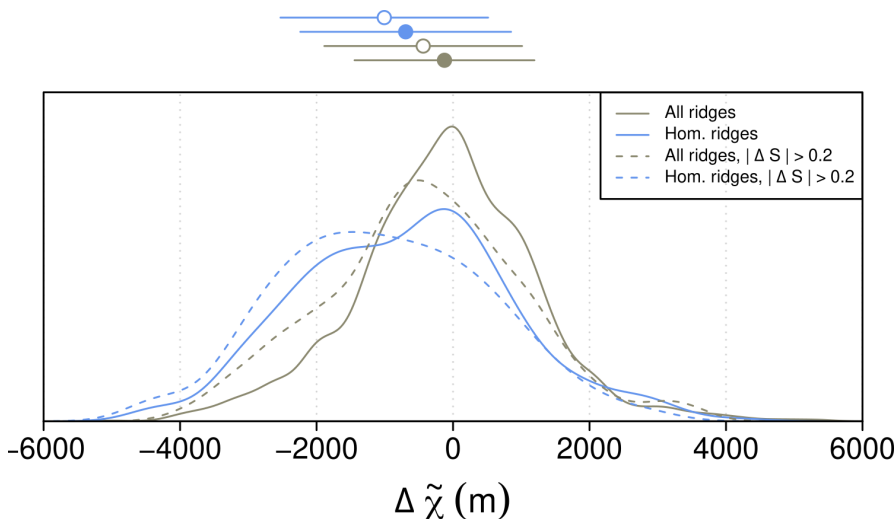


Figure 8 Kernel density estimate distributions of cross-divide differences in χ ($\Delta\tilde{\chi}$) for all extracted ridges, and for homoclinal ridges where the dip direction was identified. Note that for this figure the difference in χ across the divide ($\Delta\tilde{\chi}$) is computed from the highest to the lowest slope side, not following the dip direction (which is only defined for a limited number of ridges) as in Figs. 4 to 7. Grey and blue curves refer to the whole dataset or only the ridges where the dip direction was identified, respectively. Dashed curves are subsets for $|\Delta S| > 0.2$. On all plots the Y-axis is the estimated density, whose exact value has no particular signification.

west-oriented watershed divides, due to drastic changes in hillslope and first-order channels' dynamics between glacial and interglacial conditions. For example, the intensity of frost cracking acting on exposed cliff surfaces can change substantially and modulate the degree of imbalance between the two sides of the ridges. However, as in the cases considered above, we would expect morphometric asymmetries across the ridges to be smoothed out if this influence was dominant.

Altogether, despite the usual limitations of the computed metrics when applied to natural systems, the observed systematic asymmetry across structurally-controlled ridges in Southern France clearly supports the persistence of a structural imprint in the local and larger-scale landscape organization.

5.2 Implications for surface processes at the scale of the divide

5.2.1 Persistence of asymmetric configurations

The main deformation phases in our study area, which structured the present-day landscape, are associated with the Pyrenean and Alpine orogenies, with major shortening events during the Eocene and Miocene. Active deformation is presently very limited (Nocquet et al., 2016), and slow slipping has been identified only locally on some structures (Hippolyte and Dumont, 2000; Godard et al., 2020). While Quaternary glaciations in the upstream parts of the basins induced substantial downstream valley deepening and fluvial incision, it is clear that the bulk of the relief of these Provence and peri-Alpine ranges was acquired before the Pliocene (Bestani et al., 2016) and has been since mostly relaxing.

The idea of equilibrium for a fluvial system is a theoretical concept, especially concerning its planform organization. Events of transient mobility of ridgelines are frequent, even in the absence of changes in network scale forcing, and correspond to the internal dynamics

of the system (Hasbargen and Paola, 2000). From this perspective, it is unsurprising to still observe local differences in χ across ridges in this relaxing landscape, which was primarily deformed during the Eocene to Miocene. The key point of our study is that these differences are systematic and show a preferential relationship with local geological structures. One possibility to explain this configuration is a structural control on erosion dynamics, which could slow down migration processes and maintain the landscape out of equilibrium for extended periods of time. This asymmetry in erosive dynamics would result from the slope asymmetry across ridges, controlled by the dip of the sedimentary series. The (updip) aggressor basins would thus have their propagation rate penalized, which would induce a delay or slowdown in the possibility of the landscape to reach stability in its planform organization and from there keep it in a disequilibrium state. The persistence of an imbalance across the watersheds, and its systematic correspondence with local topographical asymmetry, can only be explained if erosion processes are less effective on the steeper (updip) side of the ridge, which may seem paradoxical from a geomorphological point of view.

Erosion rates are variable and difficult to constrain in carbonate-dominated landscapes and few estimates derived from cosmogenic nuclides are available in the investigated area, ranging from a few 10s of m/Ma to ~ 100 m/Ma (Godard et al., 2016; Thomas et al., 2017). No clear functional relationship has been calibrated between erosion rates and topographic relief or steepness. In places where erosion rates are available from both sides of a range, the amplitude of the contrast is difficult to resolve due to dispersion in the data and is probably < 100 m/Ma (Thomas et al., 2017), which suggests slow rates of lateral propagation of erosion over 10 ka timescales. It has been noted that these cosmogenic nuclides-derived divide migration rates might underestimate longer term dynamics in some contexts,

such as passive margin escarpments (Braun, 2018; Godard et al., 2019), where rapid captures of large areas of the inland low-gradient surface can drive the evolution. However, in the configurations we consider here, with narrow ridges and steeper topographic gradients even on the more gently sloping sides, this type of processes is less likely to play a dominant role. Available data on erosion rates are therefore not sufficient to document across-divide contrasts in erosion and a possible counter-intuitive slow-down of these processes in the case of the investigated steep updip slopes. However, there are situations where steep slopes can have a limiting effect on erosive processes, as we further discuss in the next sections. The key point here is that local hillslope processes, with delayed and slowed erosion on the steeper slopes of structurally-controlled asymmetric ridges, are expected to impact the associated larger fluvial network and its planform organization.

At the local scale of the structurally-controlled ridge, these processes may lead to a dynamic equilibrium, where the slow (downdip) retreat rate of the structurally-controlled cliff is steady and self-similar, as proposed for similarly layered structures such as hogbacks (Glade and Anderson, 2018). This contributes to maintain the overall shape of the ridge over time. Such local processes could imprint the overall organization of the drainage network, and contribute to a certain persistence of a larger-scale imbalance. These processes are highly dependent on the nature of weathering and transport of blocks and sediments driving the evolution of both sides of the ridge, and allows for the development of complex behavior and response timescales.

5.2.2 Controls by hillslope processes

Here, we explore and discuss some of the possible conditions and processes that may slow down erosion and weathering rates on the steepest updip side of the investigated ridges and could contribute to the persistence of the observed imbalance.

The process controlling soil production from bedrock has been a long-standing debate within the geomorphological community, and in particular the form of the Soil Production Function (SPF), which describes the rate at which bedrock is converted into soil as a function of its thickness. (Heimsath et al., 1997; Humphreys and Wilkinson, 2007). The most commonly accepted model assumes an exponential decay in this conversion rate with increasing soil thickness, reflecting the protective effect of soil cover against mechanical and chemical weathering agents (Heimsath et al., 1997, 1999). However, another model suggests that the rate of soil production does not exhibit a monotonic decrease with soil thickness, and proposes the existence of a local maximum for this function, indicating that weathering processes are more efficient in the presence of a thin regolith layer due to moisture retention or partial pressure of CO₂ within it (e.g. Furbish and Fagherazzi, 2001; Minasny et al., 2008). In other words, bare bedrock experiences lower weathering rates than areas with a thin soil layer. The thickness of the soil is also influenced by hillslope morphology as steeper slopes lead to higher

sediment fluxes, resulting in thinner soil layers. As a result, the humped model for soil production can have complex implications for erosion and weathering processes on hillslopes. For instance, slopes with steep gradients and thin soil layers could ultimately experience less active weathering than slopes with gentler gradients and thicker soils. We used simple hillslope models to explore this behavior with Landlab Landscape Evolution Modelling framework (Barnhart et al., 2020). Starting from various initial slope values, we let the hillslope evolve due to non-linear sediment flux, and a weathering rate W as a function of depth z computed with the formalism proposed by Furbish and Fagherazzi (2001),

$$W(z) = W_0 \frac{1 + \kappa z}{1 + \kappa H} e^{-z/H} \quad (6)$$

Where W_0 and H are the bare bedrock production rate and the decay length-scale of weathering in the case of the exponential model, respectively. The shape of the soil production function is controlled by the parameter κ , with $\kappa = 0 \text{ m}^{-1}$ corresponding to the simple exponential model and higher values leading to non-monotonous evolution of weathering rates with depth (Fig. 9a).

In these simple models, the exponential function ($\kappa = 0 \text{ m}^{-1}$) produces the expected positive relationship between weathering and topographic gradient (figure 9b). A more complex and surprising behavior appears for $\kappa > 2 \text{ m}^{-1}$, with a non-monotonous evolution and a decrease in weathering at high initial slope values. In this situation, the decrease of weathering and erosion on steep slopes might contribute to strongly inhibit or slow down the migration of the divide from the steep to the shallow side of the ridge. Such process could contribute to limit or delay the establishment of a landscape planform equilibrium, with steep cliffs resisting the propagation of erosion. A systematic exploration of this behavior is beyond the scope of this study, but our simple models highlight possible significant implications of the humped model for weathering on landscape evolution. We also note that previous studies have already suggested the possibility of sharp changes in hillslope dynamics in carbonate lithologies (Godard et al., 2016). The transition between regimes controlled by transport-limited processes or controlled by weathering-limited processes can promote the emergence of bedrock dominated landscape and steep cliffs that are decoupled from adjacent base level variations, which could also contribute to the inhibition of divide migration.

An additional possible process slowing down erosion on the updip steeper slopes could be driven by the presence of large blocks delivered by the cliffs, and likely more abundant on the steep side of the divides. Glade et al. (2017) developed a model of hillslope dynamics in stratified landscapes, focusing on the influence of block release and evolution, and illustrating the importance of block cover for the persistence of asymmetric morphologies. In particular, they show the potential for blocks below the cliffs to protect the underlying bedrock from weathering and eroding, and from there to contribute to the slowing down of ridge retreat. An inves-

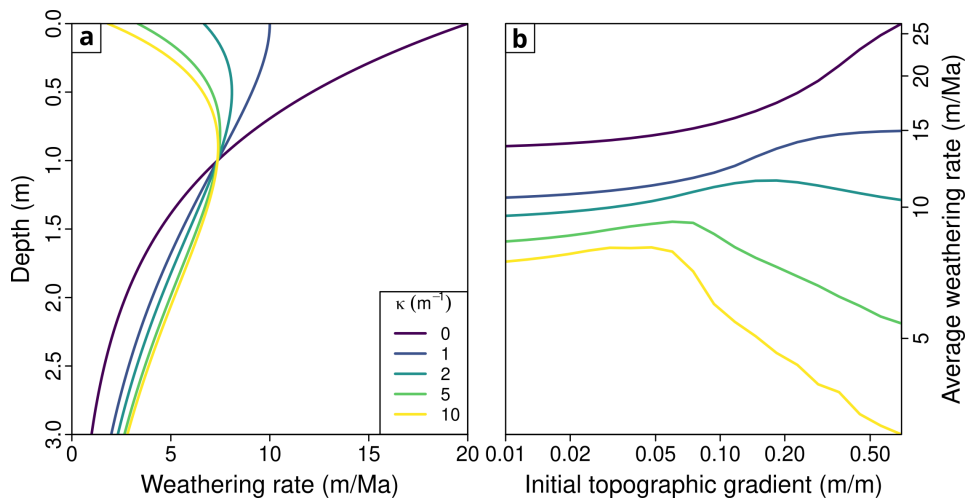


Figure 9 Simple models of hillslope evolution starting from a range of initial constant slopes. The sediment flux is controlled by a non-linear law, with transport coefficient of $0.01 \text{ m}^2/\text{a}$ and critical slope of 0.8 m/m . In equation 6 we use $H = 1 \text{ m}$ and $W_0 = 30 \text{ m/Ma}$. (a) Soil production functions for various values of the κ parameter (Furbish and Fagherazzi, 2001) controlling the shape of the function. (b) Evolution of average weathering rate along the hillslope as a function of initial slope after 1 Ma, for various values of κ .

igation of the variability in block cover across our area of interest is difficult due to dense vegetation at the foot of the cliffs, and beyond the scope of this study. We note that dense fields of metric blocks occur below the steep sides of some of the ridges, and may likely contribute to inhibit and slow down divide migration. However, there seems to be much variability from one site to the other, due probably to lithological differences, such that this effect is probably not a dominant and systematic driver of the processes we investigate.

5.2.3 Controls by channel processes

Channel incision processes can also exhibit complex dynamics depending on the slope. While the classical Stream Power model predicts that fluvial incision is strictly increasing with channel slope, more complex models based on the "tool and cover" dynamics suggest a non-monotonic relationship between incision and slope (Sklar and Dietrich, 2004). In this model, incision is primarily controlled by the probability of interaction between the sediment load being transported and the bedrock substrate of the riverbed. As the slope increases, the trajectories of transported particles, which impact the riverbed and drive incision, become longer. Consequently, a river or colluvial channel with a steep slope may not necessarily be the context where downcutting is most intense, due to the characteristics of interactions with sediment transport. For example, this mechanism has been proposed to explain the existence of hanging valleys and the decoupling of fluvial incision between a main river and its tributaries (Wobus et al., 2006). In the case of our study, it is possible that the topographic asymmetry between the two sides of the ridge also induces a difference in transport conditions in the first-order channels and colluvial systems. The reduced efficiency of incision on the steep side could contribute to the observed persistence of the imbalance (Fig. 10).

Shobe et al. (2016) explored the impact of blocks derived from adjacent hillslopes on channel incision dy-

namics. They notably identified a negative feedback where the delivery of large blocks by steep hillslopes adjacent to actively incising river reaches inhibited incision. The first order channels directly connected to the hillslopes could be sensitive to such effects. As mentioned for hillslope processes in the previous section, block-dependent processes listed here could also contribute to the slow-down in erosion processes on the steeper side of the divide.

5.3 Implications for network scale landscape evolution

Divide mobility is an intrinsic feature of landscape dynamics, which can be controlled by external forcing, but be also autogenic (Hasbargen and Paola, 2000; Bonnet, 2009). While divide mobility and planform network dynamics have been investigated with Landscape Evolution Models, most model setups have relied on the simplest form of the Stream Power formalism to represent fluvial incision. Similarly, hillslope processes are either unaccounted for or introduced using a simple linear diffusion approach. As we suggested above, considering more complex, but realistic, formulations of these processes can have unexpected implications for divide evolution, and from there for the evolution of the large-scale river network. Such processes could potentially slow down landscape evolution and maintain unstable river network configurations over millions of years. At shorter length scales, these processes could be a reason for the longevity of ridge morphological asymmetries and the persistence of pronounced cliffs in layered landscapes. Such delays can also contribute to explain the influence of structural geometries and stratigraphy in controlling the fluvial network orientation and planform structure, in addition to geometric effects already highlighted in other structurally-controlled landscapes (Ward, 2019), or in addition to the effects of local active tectonics and the related advection of rocks (e.g. Miller et al., 2007).

The timescales of landscape evolution and response

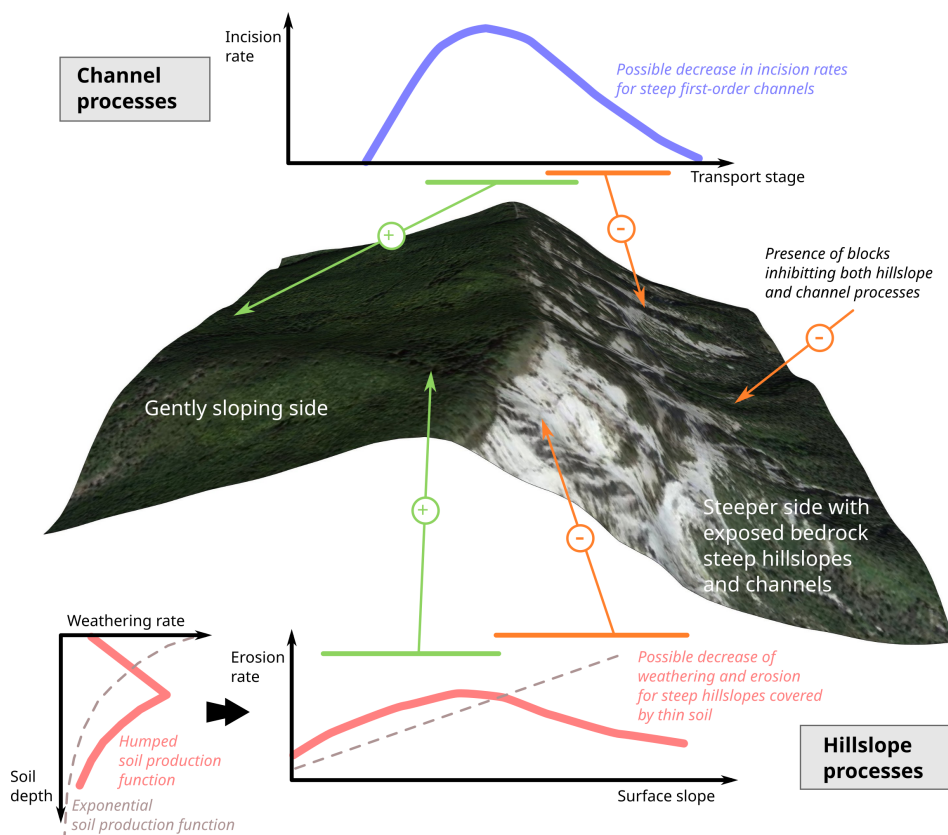


Figure 10 Conceptual summary of the possible hillslope and channel processes resulting in an inhibition of surface processes on the steeper side of an asymmetric ridge.

to perturbations are at first order dictated by the efficiency of fluvial and hillslope processes (Whipple, 2001; Roering et al., 2001). The phenomenon we investigate highlights other possible complex controls on these response times, which also introduce an asymmetry in landscape response. A detailed investigation of the physics of the processes is beyond the scope of this study, where we limit our analysis to a general discussion of the existence of such processes. Carrying out this analysis would require advanced Landscape Evolution Models, allowing to take into account layered and deformed lithological series, as well as a more complex representation of both fluvial and hillslope erosion processes.

6 Conclusion

Asymmetric ridges are common features of landscapes resulting from thin-skinned deformation of sedimentary series, even long after tectonic deformation has significantly slowed or ceased. Their morphology often displays a persistent strong structural control, with steep cliff faces on one side and gentler slopes whose gradient is set by strata dip angle on the other side. We have analyzed metrics related to ridge asymmetry and drainage divide instability in the case of the French Southern Alps, which resulted from the deformation of Mesozoic sedimentary series during the Eocene and Miocene. As expected in this landscape resulting from complex geological and past tectonic history, we observe significant χ and slope contrasts between basins from both sides of these ridges. Our key finding is that

these contrasts display a clear preferential polarity, with low χ values more likely to be located on the steep up-dip side of the ridge when χ asymmetry is present across a divide.

One could argue that these contrasts in χ and slope across ridges are consistent with predictions of drainage divide migration in non-layered landscapes and the definition of the Gilbert metrics. However, it is fundamental to keep in mind that the difference in steepness across the divide is here a structurally inherited feature, and does not result from an erosional response triggered by external factors. From that point of view, the over-representation of aggressor basins on the steep side of the divide can be interpreted as a manifestation of a delayed relaxation of the network planform toward an equilibrium configuration. We propose that this delay may arise from an inhibition of fluvial or hillslope local erosion processes on the steepest sides of the divide. This behavior can have a meaningful impact on the long-term and larger-scale evolution of these landscapes, by slowing down the relaxation of their planform structure toward an equilibrium configuration over 1 to 10 Ma timescales.

Acknowledgements

We thank the associate editor and two anonymous reviewers for constructive and insightful comments.

Native Land Recognition

This section is not relevant for the case of our study.

Data and Codes Availability

The code used in this study is available in the following Zenodo repository [10.5281/zenodo.14775163](https://doi.org/10.5281/zenodo.14775163).

Funding Statement

This research was supported by an IUF fellowship to VG and by the Agence Nationale de la Recherche through the Topo-Extreme project (ANR18-CE01-0017 grant to RC and VG). Through the work of MS, this study has been partly supported by IdEx Université de Paris ANR-18-IDEX-0001.

Conflict of Interest Disclosure

The authors have no competing interests.

Permission to Reproduce Material from Copyrighted Sources

The authors declare that no material from copyrighted sources was reproduced in this manuscript.

References

- Barnhart, K. R., Hutton, E. W. H., Tucker, G. E., Gasparini, N. M., Isitanbulluoglu, E., Hobley, D. E. J., Lyons, N. J., Mouchene, M., Nudurupati, S. S., Adams, J. M., and Bandaragoda, C. Short Communication: Landlab v2.0: A Software Package for Earth Surface Dynamics. *Earth Surface Dynamics*, 8(2):379–397, May 2020. doi: [10.5194/esurf-8-379-2020](https://doi.org/10.5194/esurf-8-379-2020).
- Bestani, L., Espurt, N., Lamarche, J., Bellier, O., and Hollender, F. Reconstruction of the Provence Chain Evolution, Southeastern France. *Tectonics*, 35(6):1506–1525, 2016. doi: [10.1002/2016TC004115](https://doi.org/10.1002/2016TC004115).
- Bivand, R. *Rgrass: Interface between 'GRASS' Geographical Information System and 'R'*, 2023.
- Bonnet, S. Shrinking and Splitting of Drainage Basins in Orogenic Landscapes from the Migration of the Main Drainage Divide. *Nature Geoscience*, 2(11):766–771, Oct. 2009. doi: [10.1038/ngeo666](https://doi.org/10.1038/ngeo666).
- Braun, J. A Review of Numerical Modeling Studies of Passive Margin Escarpments Leading to a New Analytical Expression for the Rate of Escarpment Migration Velocity. *Gondwana Research*, 53: 209–224, Jan. 2018. doi: [10.1016/j.gr.2017.04.012](https://doi.org/10.1016/j.gr.2017.04.012).
- Bursztyn, N., Pederson, J., Tressler, C., Mackley, R., and Mitchell, K. Rock Strength along a Fluvial Transect of the Colorado Plateau – Quantifying a Fundamental Control on Geomorphology. *Earth and Planetary Science Letters*, 429:90–100, 2015. doi: [10.1016/j.epsl.2015.07.042](https://doi.org/10.1016/j.epsl.2015.07.042).
- Cassemiro, F. A. S., Albert, J. S., Antonelli, A., Menegotto, A., Wüest, R. O., Cerezer, F., Coelho, M. T. P., Reis, R. E., Tan, M., Taglia-collo, V., Bailly, D., Da Silva, V. F. B., Frota, A., Da Graça, W. J., Ré, R., Ramos, T., Oliveira, A. G., Dias, M. S., Colwell, R. K., Rangel, T. F., and Graham, C. H. Landscape Dynamics and Diversification of the Megadiverse South American Freshwater Fish Fauna. *Proceedings of the National Academy of Sciences*, 120(2): e2211974120, Jan. 2023. doi: [10.1073/pnas.2211974120](https://doi.org/10.1073/pnas.2211974120).
- Clark, M. K., Schoenbohm, L. M., Royden, L. H., Whipple, K. X., Burchfiel, B. C., Zhang, W., Tang, W., Wang, E., and Chen, L. Surface Uplift, Tectonics, and Erosion of Eastern Tibet from Large-scale Drainage Patterns. *Tectonics*, 23(1):TC1006, Jan. 2004. doi: [10.1029/2002TC001402](https://doi.org/10.1029/2002TC001402).
- Clauzon, G., Aguilar, J. P., and Michaux, J. Investigation of the Time-Sedimentation Relation Thanks to Examples Taken from the French Mediterranean Neogene. *Bulletin de la Société Géologique de France*, V(2):361–372, Mar. 1989. doi: [10.2113/gssgbull.V.2.361](https://doi.org/10.2113/gssgbull.V.2.361).
- Clauzon, G., Fleury, T. J., Bellier, O., Molliex, S., Mocochain, L., and Aguilar, J. P. Morphostructural Evolution of the Luberon since the Miocene (SE France). *Bulletin de la Société Géologique de France*, 182(2):95–110, 2011. doi: [10.2113/gssgbull.182.2.95](https://doi.org/10.2113/gssgbull.182.2.95).
- Dahlquist, M. P., West, A. J., and Li, G. Landslide-Driven Drainage Divide Migration. *Geology*, 46(5):1–4, Feb. 2018. doi: [10.1130/G39916.1](https://doi.org/10.1130/G39916.1).
- Espurt, N., Hippolyte, J.-C., Saillard, M., and Bellier, O. Geometry and Kinematic Evolution of a Long-Living Foreland Structure Inferred from Field Data and Cross Section Balancing, the Sainte-Victoire System, Provence, France: STRUCTURE OF THE SAINTE-VICTOIRE SYSTEM. *Tectonics*, 31(4):n/a–n/a, Aug. 2012. doi: [10.1029/2011TC002988](https://doi.org/10.1029/2011TC002988).
- Forte, A. M. and Whipple, K. X. Criteria and Tools for Determining Drainage Divide Stability. *Earth and Planetary Science Letters*, 493:102–117, 2018. doi: [10.1016/j.epsl.2018.04.026](https://doi.org/10.1016/j.epsl.2018.04.026).
- Forte, A. M., Yanites, B. J., and Whipple, K. X. Complexities of Landscape Evolution during Incision through Layered Stratigraphy with Contrasts in Rock Strength. *Earth Surface Processes and Landforms*, 41(12):1736–1757, 2016. doi: [10.1002/esp.3947](https://doi.org/10.1002/esp.3947).
- Furbish, D. J. and Fagherazzi, S. Stability of Creeping Soil and Implications for Hillslope Evolution. *Water Resources Research*, 37 (10):2607–2618, Oct. 2001. doi: [10.1029/2001WR000239](https://doi.org/10.1029/2001WR000239).
- Gailleton, B., Mudd, S. M., Clubb, F. J., Grieve, S. W. D., and Hurst, M. D. Impact of Changing Concavity Indices on Channel Steepness and Divide Migration Metrics. *Journal of Geophysical Research: Earth Surface*, 126(10):e2020JF006060, 2021. doi: [10.1029/2020JF006060](https://doi.org/10.1029/2020JF006060).
- Gallen, S. F. Lithologic Controls on Landscape Dynamics and Aquatic Species Evolution in Post-Orogenic Mountains. *Earth and Planetary Science Letters*, 493:150–160, July 2018. doi: [10.1016/j.epsl.2018.04.029](https://doi.org/10.1016/j.epsl.2018.04.029).
- García-Delgado, H., Schwanghart, W., Hoke, G. D., Guerrero, B., and Velandia, F. How Erosional Efficiency Modulates Landscape Response to Drainage Reorganization: New Empirical Evidence from the Andes. *Geomorphology*, 440:108893, Nov. 2023. doi: [10.1016/j.geomorph.2023.108893](https://doi.org/10.1016/j.geomorph.2023.108893).
- Glade, R. C. and Anderson, R. S. Quasi-Steady Evolution of Hillslopes in Layered Landscapes: An Analytic Approach. *Journal of Geophysical Research: Earth Surface*, 123(1):26–45, 2018. doi: [10.1002/2017JF004466](https://doi.org/10.1002/2017JF004466).
- Glade, R. C., Anderson, R. S., and Tucker, G. E. Block-Controlled Hillslope Form and Persistence of Topography in Rocky Landscapes. *Geology*, 2017. doi: [10.1130/G38665.1](https://doi.org/10.1130/G38665.1).
- Godard, V., Lavé, J., Carcaillet, J., Cattin, R., Bourlès, D., and Zhu, J. Spatial Distribution of Denudation in Eastern Tibet and Regressive Erosion of Plateau Margins. *Tectonophysics*, 491(1-4): 253–274, Aug. 2010. doi: [10.1016/j.tecto.2009.10.026](https://doi.org/10.1016/j.tecto.2009.10.026).
- Godard, V., Ollivier, V., Bellier, O., Miramont, C., Shabanian, E., Fleury, J., Benedetti, L., and Guillou, V. Weathering-Limited Hillslope Evolution in Carbonate Landscapes. *Earth and Planetary Science Letters*, 446:10–20, July 2016. doi: [10.1016/j.epsl.2016.04.017](https://doi.org/10.1016/j.epsl.2016.04.017).
- Godard, V., Dosseto, A., Fleury, J., Bellier, O., Siame, L., and ASTER, T. Transient Landscape Dynamics across the Southeastern Australian Escarpment. *Earth and Planetary Science Letters*, 506:

- 397–406, Jan. 2019. doi: [10.1016/j.epsl.2018.11.017](https://doi.org/10.1016/j.epsl.2018.11.017).
- Godard, V., Hippolyte, J.-C., Cushing, E., Espurt, N., Fleury, J., Bellier, O., Ollivier, V., and ASTER, T. Hillslope Denudation and Morphologic Response to a Rock Uplift Gradient. *Earth Surface Dynamics*, 8(2):221–243, Apr. 2020. doi: [10.5194/esurf-8-221-2020](https://doi.org/10.5194/esurf-8-221-2020).
- GRASS Development Team. *Geographic Resources Analysis Support System (GRASS GIS) Software, Version 8.2*, 2022.
- Habousha, K., Goren, L., Nativ, R., and Gruber, C. Plan-Form Evolution of Drainage Basins in Response to Tectonic Changes: Insights From Experimental and Numerical Landscapes. *Journal of Geophysical Research: Earth Surface*, 128(3):e2022JF006876, 2023. doi: [10.1029/2022JF006876](https://doi.org/10.1029/2022JF006876).
- Hasbargen, L. and Paola, C. Landscape Instability in an Experimental Drainage Basin. *Geology*, 28(12):1,61–67,70, 2000. doi: [10.1130/0091-7613\(2000\)28<1067:LIAED>2.0.CO;2](https://doi.org/10.1130/0091-7613(2000)28<1067:LIAED>2.0.CO;2).
- Heimsath, A. M., Dietrich, W. E., Nishiizumi, K., and Finkel, R. C. The Soil Production Function and Landscape Equilibrium. *Nature*, 388(6640):358–361, July 1997. doi: [10.1038/41056](https://doi.org/10.1038/41056).
- Heimsath, A. M., E. Dietrich, W., Nishiizumi, K., and Finkel, R. C. Cosmogenic Nuclides, Topography, and the Spatial Variation of Soil Depth. *Geomorphology*, 27(1):151–172, Feb. 1999. doi: [10.1016/S0169-555X\(98\)00095-6](https://doi.org/10.1016/S0169-555X(98)00095-6).
- Hijmans, R. J. *Terra: Spatial Data Analysis*, 2023.
- Hippolyte, J.-C. and Dumont, T. Identification of Quaternary Thrusts, Folds and Faults in a Low Seismicity Area: Examples in the Southern Alps (France). *Terra Nova*, 12(4):156–162, 2000. doi: [10.1046/j.1365-3121.2000.00287.x](https://doi.org/10.1046/j.1365-3121.2000.00287.x).
- Howard, A. D. A Detachment-Limited Model of Drainage Basin Evolution. *Water Resources Research*, 30(7):2261–2285, 1994. doi: [10.1029/94WR00757](https://doi.org/10.1029/94WR00757).
- HSÜ, K. J., Montadert, L., Bernoulli, D., Cita, M. B., Erickson, A., Garrison, R. E., Kidd, R. B., Mèlierés, F., Müller, C., and Wright, R. History of the Mediterranean Salinity Crisis. *Nature*, 267(5610):399–403, June 1977. doi: [10.1038/267399a0](https://doi.org/10.1038/267399a0).
- Humphreys, G. S. and Wilkinson, M. T. The Soil Production Function: A Brief History and Its Rediscovery. *Geoderma*, 139(1-2):73–78, Apr. 2007. doi: [10.1016/j.geoderma.2007.01.004](https://doi.org/10.1016/j.geoderma.2007.01.004).
- Lavé, J. and Avouac, J. P. Fluvial Incision and Tectonic Uplift across the Himalayas of Central Nepal. *Journal of Geophysical Research*, 106(B11):26561–26591, 2001. doi: [10.1029/2001JB000359](https://doi.org/10.1029/2001JB000359).
- Leonide, P., Floquet, M., and Villier, L. Interaction of Tectonics, Eustasy, Climate and Carbonate Production on the Sedimentary Evolution of an Early/Middle Jurassic Extensional Basin (Southern Provence Sub-basin, SE France). *Basin Research*, 19(1):125–152, Jan. 2007. doi: [10.1111/j.1365-2117.2007.00316.x](https://doi.org/10.1111/j.1365-2117.2007.00316.x).
- Leonide, P., Borgomano, J., Masse, J.-P., and Doublet, S. Relation between Stratigraphic Architecture and Multi-Scale Heterogeneities in Carbonate Platforms: The Barremian–Lower Aptian of the Monts de Vaucluse, SE France. *Sedimentary Geology*, 265–266:87–109, July 2012. doi: [10.1016/j.sedgeo.2012.03.019](https://doi.org/10.1016/j.sedgeo.2012.03.019).
- Lyons, N. J., Val, P., Albert, J. S., Willenbring, J. K., and Gasparini, N. M. Topographic Controls on Divide Migration, Stream Capture, and Diversification in Riverine Life. *Earth Surface Dynamics*, 8(4):893–912, Oct. 2020. doi: [10.5194/esurf-8-893-2020](https://doi.org/10.5194/esurf-8-893-2020).
- Miller, S. R., Slingerland, R. L., and Kirby, E. Characteristics of Steady State Fluvial Topography above Fault-Bend Folds. *Journal of Geophysical Research: Earth Surface*, 112(F4), 2007. doi: [10.1029/2007JF000772](https://doi.org/10.1029/2007JF000772).
- Minasny, B., McBratney, Alex. B., and Salvador-Blanes, S. Quantitative Models for Pedogenesis – A Review. *Geoderma*, 144(1-2):140–157, Mar. 2008. doi: [10.1016/j.geoderma.2007.12.013](https://doi.org/10.1016/j.geoderma.2007.12.013).
- Mitchell, N. and Forte, A. M. Tectonic Advection of Contacts Enhances Landscape Transience. *Earth Surface Processes and Landforms*, 48(7):1450–1469, 2023. doi: [10.1002/esp.5559](https://doi.org/10.1002/esp.5559).
- Mollieix, S., Bellier, O., Terrier, M., Lamarche, J., Martelet, G., and Espurt, N. Tectonic and Sedimentary Inheritance on the Structural Framework of Provence (SE France): Importance of the Salon-Cavaillon Fault. *Tectonophysics*, 501(1-4):1–16, Mar. 2011. doi: [10.1016/j.tecto.2010.09.008](https://doi.org/10.1016/j.tecto.2010.09.008).
- Montgomery, D. R. and Brandon, M. T. Topographic Controls on Erosion Rates in Tectonically Active Mountain Ranges. *Earth and Planetary Science Letters*, 201(3-4):481–489, 2002. doi: [10.1016/S0012-821X\(02\)00725-2](https://doi.org/10.1016/S0012-821X(02)00725-2).
- Nocquet, J.-M., Sue, C., Walpersdorf, A., Tran, T., Lenôtre, N., Vernant, P., Cushing, M., Jouanne, F., Masson, F., Baize, S., Chéry, J., and van der Beek, P. A. Present-Day Uplift of the Western Alps. *Scientific Reports*, 6(1):28404, June 2016. doi: [10.1038/srep28404](https://doi.org/10.1038/srep28404).
- Ouimet, W. B., Whipple, K. X., and Granger, D. E. Beyond Threshold Hillslopes: Channel Adjustment to Base-Level Fall in Tectonically Active Mountain Ranges. *Geology*, 37(7):579–582, June 2009. doi: [10.1130/G30013A.1](https://doi.org/10.1130/G30013A.1).
- Pelletier, J. D. Persistent Drainage Migration in a Numerical Landscape Evolution Model. *Geophysical Research Letters*, 31(20):L20501, Oct. 2004. doi: [10.1029/2004GL020802](https://doi.org/10.1029/2004GL020802).
- Perron, J. T. and Royden, L. An Integral Approach to Bedrock River Profile Analysis. *Earth Surface Processes and Landforms*, 38(6):570–576, 2013. doi: [10.1002/esp.3302](https://doi.org/10.1002/esp.3302).
- Perron, J. T., Dietrich, W. E., and Kirchner, J. W. Controls on the Spacing of First-Order Valleys. *Journal of Geophysical Research*, 113(F4):F04016, Dec. 2008. doi: [10.1029/2007JF000977](https://doi.org/10.1029/2007JF000977).
- Perron, J. T., Richardson, P. W., Ferrier, K. L., and Lapôtre, M. The Root of Branching River Networks. *Nature*, 492(7427):100–103, Dec. 2012. doi: [10.1038/nature11672](https://doi.org/10.1038/nature11672).
- R Core Team. *R: A Language and Environment for Statistical Computing*. Vienna, Austria, 2023.
- Roering, J. J., Kirchner, J. W., and Dietrich, W. E. Hillslope Evolution by Nonlinear, Slope-Dependent Transport: Steady State Morphology and Equilibrium Adjustment Timescales. *Journal of Geophysical Research*, 106(B8):16499–16513, 2001. doi: [10.1029/2001JB9000323](https://doi.org/10.1029/2001JB9000323).
- Rohrmann, A., Kirby, E., and Schwanghart, W. Accelerated Miocene Incision along the Yangtze River Driven by Headward Drainage Basin Expansion. *Science Advances*, 9(36):eadh1636, Sept. 2023. doi: [10.1126/sciadv.adh1636](https://doi.org/10.1126/sciadv.adh1636).
- Sassolas-Serrayet, T., Cattin, R., Ferry, M., Godard, V., and Simoes, M. Estimating the Disequilibrium in Denudation Rates Due to Divide Migration at the Scale of River Basins. *Earth Surface Dynamics*, 7(4):1041–1057, Nov. 2019. doi: [10.5194/esurf-7-1041-2019](https://doi.org/10.5194/esurf-7-1041-2019).
- Scherler, D. and Schwanghart, W. Drainage Divide Networks - Part 1: Identification and Ordering in Digital Elevation Models. *Earth Surface Dynamics*, 8(2):245–259, 2020. doi: [10.5194/esurf-8-245-2020](https://doi.org/10.5194/esurf-8-245-2020).
- Schwanghart, W. and Scherler, D. Divide Mobility Controls Knick-point Migration on the Roan Plateau (Colorado, USA). *Geology*, 48(7):1–5, Apr. 2020. doi: [10.1130/G47054.1](https://doi.org/10.1130/G47054.1).
- Shobe, C. M., Tucker, G. E., and Anderson, R. S. Hillslope-Derived Blocks Retard River Incision. *Geophysical Research Letters*, 43(10):5070–5078, 2016. doi: [10.1002/2016GL069262](https://doi.org/10.1002/2016GL069262).
- Sklar, L. S. and Dietrich, W. E. A Mechanistic Model for River Incision into Bedrock by Saltating Bed Load. *Water Resources Research*, 40(6):W06301, June 2004. doi: [10.1029/2003WR002496](https://doi.org/10.1029/2003WR002496).
- Small, E. E., Blom, T., Hancock, G. S., Hynek, B. M., and Wobus, C. W.

- Variability of Rock Erodibility in Bedrock-Floored Stream Channels Based on Abrasion Mill Experiments. *Journal of Geophysical Research: Earth Surface*, 120(8):1455–1469, Aug. 2015. doi: [10.1002/2015JF003506](https://doi.org/10.1002/2015JF003506).
- Stark, C. P. Oscillatory Motion of Drainage Divides. *Geophysical Research Letters*, 37(4):L04401, Feb. 2010. doi: [10.1029/2009GL040851](https://doi.org/10.1029/2009GL040851).
- Thomas, F., Godard, V., Bellier, O., Shabanian, E., Ollivier, V., Benedetti, L., Rizza, M., Espurt, N., Guillou, V., Hollender, F., and Molliex, S. Morphological Controls on the Dynamics of Carbonate Landscapes under a Mediterranean Climate. *Terra Nova*, 29 (3):173–182, June 2017. doi: [10.1111/ter.12260](https://doi.org/10.1111/ter.12260).
- Tucker, G. E. and Whipple, K. X. Topographic Outcomes Predicted by Stream Erosion Models: Sensitivity Analysis and Intermodel Comparison. *Journal of Geophysical Research*, 107(B9):2179, Sept. 2002. doi: [10.1029/2000JB000044](https://doi.org/10.1029/2000JB000044).
- Vacherat, A., Bonnet, S., and Mouthereau, F. Drainage Reorganization and Divide Migration Induced by the Excavation of the Ebro Basin (NE Spain). *Earth Surface Dynamics*, 6(2):369–387, May 2018. doi: [10.5194/esurf-6-369-2018](https://doi.org/10.5194/esurf-6-369-2018).
- Val, P., Lyons, N. J., Gasparini, N., Willenbring, J. K., and Albert, J. S. Landscape Evolution as a Diversification Driver in Freshwater Fishes. *Frontiers in Ecology and Evolution*, 9, Jan. 2022. doi: [10.3389/fevo.2021.788328](https://doi.org/10.3389/fevo.2021.788328).
- Walpersdorf, A., Sue, C., Baize, S., Cotte, N., Bascou, P., Beauval, C., Collard, P., Daniel, G., Dyer, H., Grasso, J. R., Hautecoeur, O., Helmstetter, A., Hok, S., Langlais, M., Menard, G., Mousavi, Z., Ponton, F., Rizza, M., Rolland, L., Souami, D., Thirard, L., Vaudey, P., Voisin, C., and Martinod, J. Coherence between Geodetic and Seismic Deformation in a Context of Slow Tectonic Activity (SW Alps, France). *Journal of Geodynamics*, 85:58–65, 2015. doi: [10.1016/j.jog.2015.02.001](https://doi.org/10.1016/j.jog.2015.02.001).
- Ward, D. J. Dip, Layer Spacing, and Incision Rate Controls on the Formation of Strike Valleys, Cuestas, and Cliffbands in Heterogeneous Stratigraphy. *Lithosphere*, 11(5):697–707, 2019. doi: [10.1130/L1079.1](https://doi.org/10.1130/L1079.1).
- Waters, J. M., Craw, D., Youngson, J. H., and Wallis, G. P. Genes Meet Geology: Fish Phylogeographic Pattern Reflects Ancient, Rather than Modern, Drainage Connections. *Evolution*, 55(9):1844–1851, Sept. 2001. doi: [10.1111/j.0014-3820.2001.tb00833.x](https://doi.org/10.1111/j.0014-3820.2001.tb00833.x).
- Whipple, K. X. Fluvial Landscape Response Time: How Plausible Is Steady-State Denudation? *American Journal of Science*, 301 (4-5):313–325, Apr. 2001. doi: [10.2475/ajs.301.4-5.313](https://doi.org/10.2475/ajs.301.4-5.313).
- Whipple, K. X. The Influence of Climate on the Tectonic Evolution of Mountain Belts. *Nature Geoscience*, 2(2):97–104, Jan. 2009. doi: [10.1038/ngeo413](https://doi.org/10.1038/ngeo413).
- Whipple, K. X. and Tucker, G. E. Dynamics of the Stream-Power River Incision Model: Implications for Height Limits of Mountain Ranges, Landscape Response Timescales, and Research Needs. *Journal of Geophysical Research*, 104(B8):17661–17674, Aug. 1999. doi: [10.1029/1999JB900120](https://doi.org/10.1029/1999JB900120).
- Whipple, K. X., DiBiase, R. A., Ouimet, W. B., and Forte, A. M. Preservation or Piracy: Diagnosing Low-Relief, High-Elevation Surface Formation Mechanisms. *Geology*, 44(1):G38490.1, Nov. 2016. doi: [10.1130/G38490.1](https://doi.org/10.1130/G38490.1).
- Whipple, K. X., Forte, A. M., DiBiase, R. A., Gasparini, N. M., and Ouimet, W. B. Timescales of Landscape Response to Divide Migration and Drainage Capture: Implications for the Role of Divide Mobility in Landscape Evolution. *Journal of Geophysical Research: Earth Surface*, 122(1):248–273, 2017. doi: [10.1002/2016JF003973](https://doi.org/10.1002/2016JF003973).
- Whittaker, A. C. How Do Landscapes Record Tectonics and Climate? *Lithosphere*, 4:160–164, 2012. doi: [10.1130/L003.1](https://doi.org/10.1130/L003.1).
- Willett, S. D., McCoy, S. W., Perron, J. T., Goren, L., and Chen, C.-Y. Dynamic Reorganization of River Basins. *Science*, 343(6175): 1248765, Mar. 2014. doi: [10.1126/science.1248765](https://doi.org/10.1126/science.1248765).
- Wobus, C. W., Crosby, B. T., and Whipple, K. X. Hanging Valleys in Fluvial Systems: Controls on Occurrence and Implications for Landscape Evolution. *Journal of Geophysical Research: Earth Surface*, 111(2):1–14, 2006. doi: [10.1029/2005JF000406](https://doi.org/10.1029/2005JF000406).
- Zhou, C. and Tan, X. Quantifying the Influence of Asymmetric Uplift, Base Level Elevation, and Erodibility on Cross-Divide Chi Difference. *Geomorphology*, 427:108634, Apr. 2023. doi: [10.1016/j.geomorph.2023.108634](https://doi.org/10.1016/j.geomorph.2023.108634).
- Zhou, C., Tan, X., Liu, Y., Lu, R., Murphy, M. A., He, H., Han, Z., and Xu, X. Ongoing Westward Migration of Drainage Divides in Eastern Tibet, Quantified from Topographic Analysis. *Geomorphology*, 402:108123, Apr. 2022. doi: [10.1016/j.geomorph.2022.108123](https://doi.org/10.1016/j.geomorph.2022.108123).
- Zondervan, J. R., Whittaker, A. C., Bell, R. E., Watkins, S. E., Brooke, S. A. S., and Hann, M. G. New Constraints on Bedrock Erodibility and Landscape Response Times Upstream of an Active Fault. *Geomorphology*, 351:106937, Feb. 2020. doi: [10.1016/j.geomorph.2019.106937](https://doi.org/10.1016/j.geomorph.2019.106937).

The article *Influences of structurally-controlled ridge asymmetry on drainage network and divide dynamics* © 2024 by Godard et al. is licensed under a [Creative Commons Attribution 4.0 International \(CC BY 4.0\) License](https://creativecommons.org/licenses/by/4.0/).